

Conclusions

The present ab initio survey of dodecahedrane inclusion compounds offers no promise of special stability for these systems. The neutral species are unstable, and only limited stability is found for the included ions, which are essentially "unsolvated" by the hydrocarbon framework. Perhaps the most promising candidate is $C_{20}H_{20}Be^{2+}$ which is stable relative to dissociation by -170 kcal/mol. However, just as relevant as the energy is the probable large barrier to inward and outward passage. Thus, the beryllium would have to be synthesized "in situ" and would thereafter remain inside the dodecahedron.

An interesting question regarding $C_{20}H_{21}^+$ (and the other cations) is the role of electrostatic vs. covalent stabilization. The total stabilization energy of $C_{20}H_{21}^+$ with the hydrogen at the center is -42.4 kcal/mol. An SCF calculation was performed with a bare proton (i.e., without basis functions) at the center and it

furnished a stabilization energy of only 10.7 kcal/mol. Since this energy includes both electrostatic and charge-induction energies,¹¹ the bulk of the proton affinity appears to be covalent in origin.

It is interesting to point out that the induction energy does not include charge-induced dipole interactions. As we have previously shown,¹ the lowest nonvanishing permanent moment of dodecahedrane is its 2^6 -pole moment. Since the perturbing proton does not lower the I_h symmetry of the system, the induced moment can also be no lower than order 2^6 .

Acknowledgment. One of us (J.M.S.) is pleased to acknowledge a grant in aid from the CUNY Research Foundation.

(11) The STO-3G basis set furnished a polarizability of 13.7×10^{-24} cm³, which is about half that expected from empirical bond polarizability values. We have found similar STO-3G underestimates of polarizabilities in other molecules.

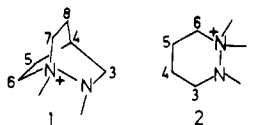
Conformational Interconversions in Pentaalkylhydrazine Cation Tetrafluoroborates

Stephen F. Nelsen* and Peter M. Gannett

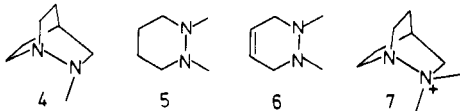
Contribution from the Samuel M. McElvain Laboratories of Organic Chemistry, Department of Chemistry, University of Wisconsin, Madison, Wisconsin 53706. Received September 15, 1980

Abstract: Peak coalescence dynamic NMR data gave the results that ΔG^\ddagger for equilibration of C_6 and C_7 in 1,2-dimethyl-1-diaza-2-azoniabicyclo[2.2.2]octane tetrafluoroborate (**1**) is 9.0 kcal/mol at -70 °C, that for N^+Me_2 interconversion in 1,1,2-trimethylhexahydropyridazinium tetrafluoroborate (**2**) is 11.1 kcal/mol at -20 °C, and that for N^+Me_2 interconversion in 1,1,2-trimethyl-1,2,3,6-tetrahydropyridazinium tetrafluoroborate is 10.4 kcal/mol at -40 °C. From broadenings at C_6 in **2** and **3** it was determined that **2** exists about 0.2 to 0.3% in the axial *N*-methyl form (-80 °C) and **3** about 3.5 to 5.5% (-80 °C). These results are interpreted to indicate that nitrogen inversion barriers are only rather weakly increased by inductive electron withdrawal, that rotational barriers in pentaalkylhydrazines lie between the "passing" and "nonpassing" barriers of the related tetraalkylhydrazines, and that the electronic energy destabilization of the *ee* relative to the *ae* form of 1,2-dimethylhexahydropyridazine (**6**) is about 2 kcal/mol.

We have carried out a dynamic carbon NMR study of conformational interconversions in pentaalkylhydrazinium tetrafluoroborates **1**–**3**. These salts were prepared by treatment of



the corresponding iodide salt (e.g., from **4** and MeI) with silver oxide and tetrafluoroboric acid, or by direct methylation of **5** and **6** with Meerwein's salt. Dimethylation was not observed under



these conditions, but **4** gave an approximately 70:30 mixture of **1** and **7**, which were separated by crystallization.

The carbon NMR shifts observed at ambient temperature, where conformational interconversion is rapid, and at low temperature, where it is slow, are shown in Table I. The rates of exchange between mirror image conformations of **1**, **2**, and **3** were determined by simulation of the NMR spectra at various temperatures, and the activation parameters calculated are summarized in Table II.

Table I. Carbon NMR Shifts for Pentaalkylhydrazine Cations (ppm Downfield from Internal Me_4Si)

| compd | ambient <i>T</i> , °C | low <i>T</i> , °C | assignment |
|----------------------|--------------------------|-------------------|--------------|
| 1^a | 49.19 | 48.74 | N_1^+Me |
| | 37.99 | 37.55 | N_2Me |
| | 58.05 | 57.58 | C_3H_2 |
| | 20.91 | 20.64 | C_4H |
| | 22.58 | 22.30 (br) | C_5, C_8 |
| | 56.03 | 50.03, 60.97 | C_6, C_7 |
| 2^b | 46.51 | 36.12, 54.29 | N_1^+Me |
| | 38.22 | 37.75 | N_2Me |
| | 50.79 | 49.95 | C_3H_2 |
| | 18.72 | 18.12 | C_4H_2 |
| | 22.24 | 22.01 | C_5H_2 |
| | 67.07 | 66.24 | C_6H_2 |
| 3^c | 46.48 | 52.12, 36.96 | N_1^+Me |
| | 37.01 | 36.53 | N_2Me |
| | 51.09 | 50.53 | C_3H_2 |
| | 116.61 | 117.42, 117.61 | C_4H, C_5H |
| | 63.21 | 62.70 | C_6H_2 |

^a Low-temperature spectrum at -102 °C. ^b At -71 °C. ^c At -86 °C.

Discussion

2-Azabicyclooctane Derivatives. The carbon assignments for **1** seem unambiguous. The two sets of two equivalent methylene carbons at ambient temperature, C_6, C_7 and C_5, C_8 , differ greatly

Table II. Conformational Barriers for the Pentaalkylhydrazine Cation Determined by Dynamic ^{13}C NMR

| compd | signals anal. | temp range, $^{\circ}\text{C}$ | ΔG^{\ddagger} , kcal/mol ^a [T_c , $^{\circ}\text{C}$] | ΔH^{\ddagger} , ^a kcal/mol | ΔS^{\ddagger} , ^a eu | ΔG^{\ddagger} , kcal/ mol ^a [25 $^{\circ}\text{C}$] |
|-------|--------------------------|--------------------------------|---|--|---|--|
| 1 | C_6, C_7 | -110 to -40 ^b | 9.01 (3) [-70] | 8.9 (e) | -0.3 (17) | 9.0 (2) |
| 2 | N_1Me_2 | -70 to +25 ^c | 11.13 (8) [-20] | 11.4 (6) | 1.1 (25) | 11.1 (2) |
| 3 | N_1Me_2 | -90 to +5 ^d | 10.40 (3) [-40] | 10.6 (2) | 1.0 (8.0) | 10.3 (1) |

^a Calculated with $\kappa = 1$. Numbers in parentheses are statistical uncertainties in the last place quoted, propagated at the 95% confidence level, and are included principally to allow comparison with earlier work.³ ^b In acetone- d_6 , eleven data points simulated. ^c In acetone- d_6 , twelve data points. ^d In acetone- d_6 -acetonitrile- d_3 (2:1 by volume), sixteen data points.

Table III. Comparison of N_2 Inversion Barriers in Some Derivatives of 2-Azabicyclo[2.2.2]octane

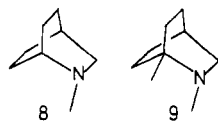
| compd (X =) | ΔG^{\ddagger} , kcal/ mol [-100 $^{\circ}\text{C}$] | ΔH^{\ddagger} , kcal/mol | ΔS^{\ddagger} , eu |
|------------------------------------|---|-------------------------------------|----------------------------|
| 8 ^a (CH) | 6.36 (10) | 7.3 (6) | +6 (4) |
| 9 ^a (CMe) | 6.49 (8) | 7.7 (9) | +7 (5) |
| 4 ^a (N:) | 7.80 (3) | 8.7 (5) | +5 (3) |
| 1 ^b (NMe ⁺) | 9.00 (5) | 8.9 (3) | 0 (2) |

^a Reference 1. ^b This work.

in chemical shift, and the downfield set is clearly that adjacent to the N_1^+ (C_6, C_7), since it freezes out to two signals differing in chemical shift by 10.9 ppm, because one methylene interacts sterically with N_2Me . A much smaller chemical shift difference, as expected, must be shown by C_5 and C_8 , for they still appear as a broadened singlet at -110 $^{\circ}\text{C}$, the lowest temperature we could use because of solubility problems. Comparison of the shifts for **1** with those for **4**¹ shows that the effect of methylating and generating a positive charge at N_1 is to cause a large downfield shift for the attached carbons (10.2 ppm for $\text{C}_{6,7}$ at ambient temperature), so the downfield methyl carbon is clearly attached to N_1^+ . Only a small downfield shift (+0.5 ppm at C_3) or modest upfield shifts (-2.4 to -4.6 ppm) are seen for the carbons not attached to N_1^+ .

The process causing the C_6, C_7 signals of **1** to coalesce at higher temperatures is rather clearly nitrogen inversion at N_2 . Although the bicyclic ring of **1** probably has significant torsion because of the unsymmetrical substitution at N_2 , the energy barrier for this torsion is expected to be much lower than that for nitrogen inversion.

A comparison of the N_2 inversion barrier of **1** with those for neutral hydrazine **4** and their amine analogues with N_1 replaced by carbon (**8** and **9**) appears in Table III. Introduction of a C_1



methyl group in going from **8** to **9** only has a small effect on the N_2 inversion barrier, but ΔG^{\ddagger} increases much more substantially when a methyl (and positive charge) is introduced at N_1 in going from **4** to **1**. The nitrogen inversion barrier increases upon going from **8** to **4**, despite the fact that lone pair, lone pair interaction effects should be eliminated at the transition state because the lone pairs are held perpendicular.¹ The inductive effect of replacing C_1 by the more electronegative N_1 might be invoked as being principally responsible for this increase because an increase in nitrogen inversion barrier when electronegative groups are attached is observed, and has been correlated with electronegativity.² The quaternary ammonium cationic N_1 of **1** is clearly more electron withdrawing than a neutral nitrogen, and if the

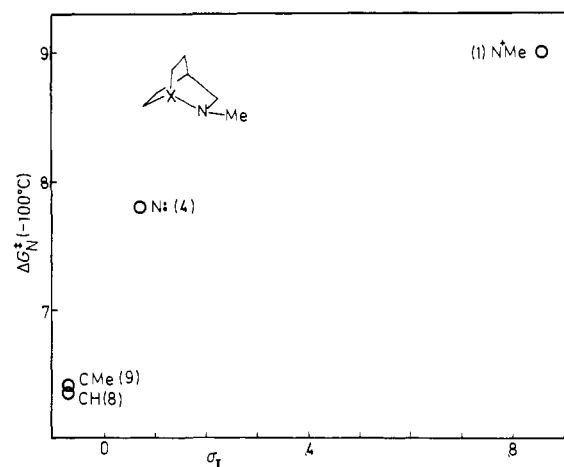


Figure 1. Plot of ΔG_N^{\ddagger} (-100 $^{\circ}\text{C}$), kcal/mol, for nitrogen inversion at N_2 vs. estimated σ_1 for the substituent position 1 for 2-methyl-2-azabicyclo[2.2.2]octane derivatives **1**, **4**, **8**, and **9**.

inductive effect is indeed important, perhaps the principal reason for a higher barrier for N_2 inversion in **1** is this effect.

To explore this possibility, we show a plot of observed barrier to nitrogen inversion ΔG_N^{\ddagger} (-100 $^{\circ}\text{C}$), kcal/mol, vs. an inductive parameter for the 1 position, employing $\sigma_1 = -0.07$ (that for *tert*-butyl) for **8** and **9**, +0.06 (that for NMe_2) for **4**, and +0.86 (that for NMe_3^+) for **1** as Figure 1. This plot emphasizes the small sensitivity of ΔG_N^{\ddagger} to the inductive effect at position 1 and suggests that the principal reason for a higher ΔG_N^{\ddagger} for hydrazine **4** than for amine **8** is not simply inductive.

Lone pair, lone pair interaction at the transition state is known to raise ΔG^{\ddagger} substantially,³ and it seems likely that all lone pair, lone pair interaction is not eliminated at the transition state, despite the formal perpendicularity of the N_1 lone pair with the p hybridized lone pair in a planar N_2 transition state for nitrogen inversion. We note that although INDO/MINDO-level calculations predict a crossing and hence a zero-energy difference between the symmetric and antisymmetric lone pair combinations when the lone pair, lone pair dihedral angle is somewhere near 85 $^{\circ}$,⁴ experimentally this crossing is avoided, as shown by the photoelectron spectra of a host of gauche tetraalkylhydrazines which cannot all have the same lone pair, lone pair dihedral angle, but all have a symmetric, antisymmetric lone pair energy gap of 0.52 ± 0.2 eV.⁵ It seems likely to us that lone pair, lone pair interaction is not totally avoided in the transition state for nitrogen inversion in **4**, and this is the principal reason for the 1.4 kcal/mol higher ΔG_N^{\ddagger} for **4** than for **8**.

1,1,2-Trimethylhexahydropyridazinium (2). The carbons β to nitrogen (C_4, C_5) of **2** are clearly those appearing at δ 18 and 22, although their assignment is not clear from our data. There are four chair conformations of **2**, since N_2 can invert and there are

(1) Nelson, S. F.; Weisman, G. R. *J. Am. Chem. Soc.* **1976**, *98*, 1842.
(2) See: Lehn, J. M. *Fortschr. Chem. Forsch.* **1971**, *15*, 311, 345-7, for a discussion.

(3) (a) Nelsen, S. F. *Acc. Chem. Res.* **1978**, *11*, 14. (b) Nelsen, S. F.; Weisman, G. R. *J. Am. Chem. Soc.* **1976**, *98*, 3281.
(4) (a) Rademacher, P. *Angew. Chem.*, **1973**, *85*, 410. (b) Nelsen, S. F.; Buschek, J. M. *J. Am. Chem. Soc.* **1973**, *95*, 2011.
(5) (a) Nelsen, S. F.; Buschek, J. M. *J. Am. Chem. Soc.* **1974**, *96*, 2392. (b) Nelsen, S. F.; Peacock, V. E.; Weisman, J. R. *Ibid.* **1976**, *98*, 5296.

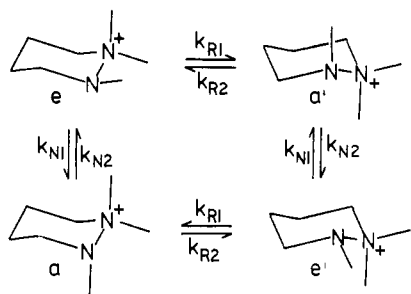


Figure 2. Conformational interconversion diagram for **2**.

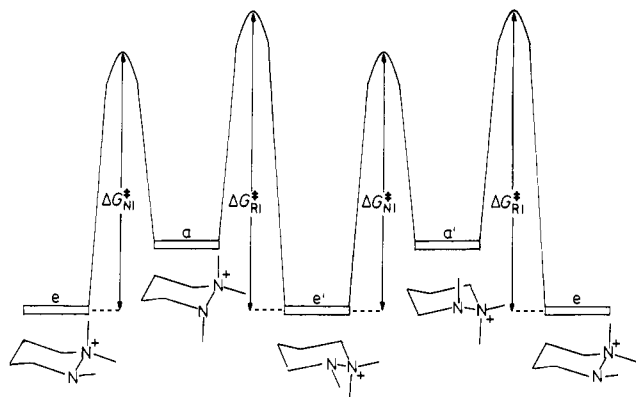
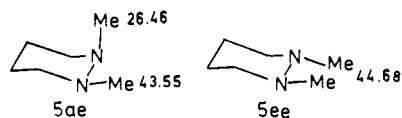


Figure 3. Energy diagram for the interconversion of **2** conformations.

two ring-reversal forms. Because of its symmetry, **2** exists in two mirror image pairs, designated *e/e'* and *a/a'*, signifying the configuration at N_2 (see Figure 2). Only one mirror image pair was observed at low temperature, which we assign as **2e/2e'**, from the N_2 Me and C_3 chemical shifts. The axial methyl of **5ae** appears over 17 ppm upfield of the equatorial methyl, and the methyls of **5ee**; carbon shifts^{3b} are shown next to the structures. If the N_2 methyl of frozen **2** were axial, its resonance would surely appear



at $\delta < 30$ (and an upfield shift at N_2 , not a downfield one, was found upon N_1 methylation of **4**, so we would expect such a methyl at $\delta < 25$); it comes at δ 37.8. Similar arguments can be made concerning the NCH_2 shifts, leading to the same conclusion, that **2e/2e'** is the observed low-temperature conformation.

As may be seen from the energy diagram in Figure 3, if either ring reversal or nitrogen inversion becomes slow on the NMR time scale, *e* will not interconvert rapidly with *e'*, and the $N_1^+Me_2$ signal will appear as two peaks. We assign the observed conformational barrier for **2** to ring reversal (ΔG^*_{R1}). The observed figure is significantly higher than the 10.2–10.3 kcal/mol barriers observed for cyclohexane, *cis*-1,2-dimethylcyclohexane, and the “nonpassing” ring reversal of **5** (**5ee'** \rightarrow **5aa**), but somewhat lower than the “passing” ring reversal of **5** (**5ae** \rightarrow **5ea'**).³ The “nonpassing” nitrogen inversion barrier **5ae** \rightarrow **5aa** is 7.6 kcal/mol ($-100^\circ C$), almost the same as the barrier for **4**, so we would not predict the nitrogen inversion barrier for **2** to be 2 kcal/mol above that for **1**, as would be required if the observed barrier for **2** were assigned to ΔG^*_{N1} .

1,1,2-Trimethyl-1,2,3,6-tetrahydropyridazinium (3). The similarity of the carbon shifts of **2** and **3** and of **5ae** and **6ae** requires that the observed low-temperature conformation of **3** is **3e/3e'**. The energy diagram for **3** resembles that in Figure 3 for **2** except that the ring reversal barrier ought to be considerably lower. The ring reversal barrier for cyclohexene is 5.4 kcal/mol ($-167^\circ C$)⁶ and that for 4,4-dimethylcyclohexene is 6.1 kcal/mol ($-156^\circ C$).⁷

We therefore attribute the 10.4 kcal/mol ($-40^\circ C$) barrier observed for **3** to nitrogen inversion, ΔG^*_{N1} . This barrier is 1.4 kcal/mol higher than that for **1**. The “nonpassing” nitrogen inversion barrier for **6**, 8.1 kcal/mol ($-87^\circ C$),⁸ is only 0.2 kcal/mol higher than that for **4**, so the introduction of a second methyl at N_1 in converting **6** to **3** raises the inversion barrier of the N_2 Me group by 2.3 kcal/mol, compared to a 1.2 kcal/mol increase for **1** vs. **4**. It seems possible that different degrees of ring torsion in **6ea** and **3e** and/or of bicyclic torsion in **4** and **1** are responsible for the rather larger increase in nitrogen inversion barriers in the monocyclic than in the bicyclic case, but we have no direct evidence on this point.

Results and Discussion. Minor Conformations of **2** and **3**

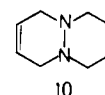
Although only **2e/2e'** and **3e/3e'** were observed at low temperature, where conformational interconversion is slow, we saw obvious evidence for the presence of **3a/3a'** conformations in the line width of the C_6 signal as the temperature was lowered. The C_6 peak started broadening below $-50^\circ C$, reached a maximum broadening at about $-80^\circ C$, and sharpened at lower temperature. As Anet and co-workers⁹ pointed out, such broadening will be seen when a minor conformation is only slightly populated, if there is a large chemical shift difference between the major and minor conformations. The population of the minor conformation at the temperature of maximum broadening, *P*, is given by the equation:

$$\nu^{(1/2\max)} = P\Delta\nu$$

where $\Delta\nu$ is the difference in shifts for the two conformations, in hertz, and $\nu^{(1/2\max)}$ is the conformationally caused broadening at half-height, in hertz. The sum of the rate constants for population and depopulation of the minor conformation at the temperature of maximum broadening is given by the equation:

$$k \text{ (s}^{-1}\text{)} = 2\pi\Delta\nu$$

Since **2** showed only barely significant broadening at C_6 , using the 25 MHz data collected for the peak coalescence work, we restudied both **2** and **3** at 50.1 MHz to get data of sufficient quality for useful application of the Anet equations. To apply these equations, values of $\Delta\nu$ must be estimated for C_6 of **2** and **3**. We estimate these values by considering model compounds **5**, **6**, and **10**. For the hexahydropyridazine **5**, **5ea** has C_6 (the carbon



interacting with the axial N_2Me) appearing 11.25 ppm upfield of C_3 , and 15.25 ppm upfield of $C_{3,6}$ for **5ee**. In the unsaturated compound **6**, C_6 of **6ea** appears 8.45 ppm upfield of C_3 (which is 0.75 times as much as in **5ea**). **6ee** could not be observed, but both forms were seen for **10**,¹⁰ where C_6 of **10ea** appears 13.2 ppm upfield of C_3 and 16.58 ppm upfield of $C_{3,6}$ of **10ee**. There is every reason to expect an axial *N*-methyl group to cause as large an upfield shift in pentaalkylhydrazine salts as in the neutral hydrazines, because in **2e**, C_3 interacting with the axial N_1^+Me appears 16.29 ppm upfield of C_6 , and the corresponding shift difference in **3e** is 12.17 ppm (0.75 times as large for the tetrahydropyridazine derivative as for the hexahydropyridazine, the same fraction as in the neutral hydrazines). We employ ranges for $\Delta\delta(C_6)$ of **2e,2a** of 14–22 ppm ($\Delta\nu$ 700–1100 Hz at 50.1 MHz) and of **3e,3a** of 11–17 ppm ($\Delta\nu$ 550–850 Hz) in this work.

Maximum conformationally caused broadening for C_6 of **3** was 26.4 Hz at $-80^\circ C$, corresponding to a population of **3a** of 3.5 to 5.5% at this temperature, and ΔG^* ($-80^\circ C$) of 7.9₃ (± 0.08) kcal/mol for the lowest barrier separating **3a** and **3e**. For **2**, the broadening reached a maximum of 2.2 Hz at $-80^\circ C$, corre-

(7) Bernard, M.; St.-Jaques, M. *Tetrahedron* **1973**, *29*, 2539.

(8) Nelsen, S. F.; Weisman, G. R. *J. Am. Chem. Soc.* **1976**, *98*, 7007.

(9) (a) Anet, F. A. L.; Yavari, I.; Ferguson, I. J.; Katritsky, A. R.; Mor-enz-Manas, M.; Robinson, M. T. *J. Chem. Soc., Chem. Commun.* **1976**, 399. (b) Anet, F. A. L.; Basus, V. J. *J. Magn. Reson.* **1978**, *32*, 339.

(10) Nelsen, S. F.; Clennan, E. L. *J. Am. Chem. Soc.* **1978**, *100*, 4004.

(6) Jensen, F. R.; Bushweller, C. H. *J. Am. Chem. Soc.* **1969**, *91*, 5744.

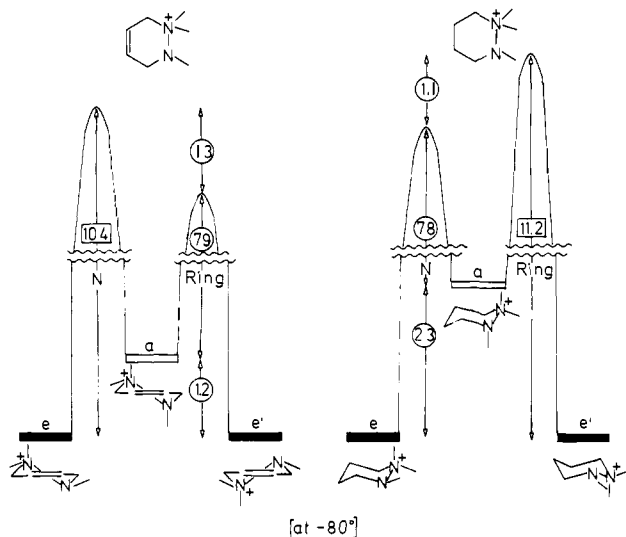


Figure 4. Relative energies of ground state and transition states at $-80\text{ }^{\circ}\text{C}$ for **2** (at right) and **3** (at left). Numbers derived from $e \rightleftharpoons e'$ peak coalescence are shown in squares, and those from broadening at C_6 , using the Anet equations, are shown in circles.

sponding to a population of **2a** of 0.2 to 0.3%, and ΔG^{\ddagger} ($-80\text{ }^{\circ}\text{C}$) of 7.8_3 (± 0.08) kcal/mol. When combined with the $e \rightleftharpoons e'$ coalescence data of Table II (extrapolated to $-80\text{ }^{\circ}\text{C}$), the relative energies shown in Figure 4 are derived.

The relative energies in Figure 4 are quite consistent both with the peak coalescence measurements and expectations from related work. A higher **2a,2e** ground state energy gap than the **3a,3e** gap (2.3 vs. 1.2 kcal/mol) is entirely consistent with removal of one axial ring hydrogen in going from **2** to **3**. The 2.3 kcal/mol destabilization of **2a** relative to **2e** is also reasonable compared with the 2.7 kcal/mol destabilization of axial vs. equatorial *N*-methylpiperidine.^{9a,11} The adjacent methyl at N_1 of **2e** should introduce some steric destabilization relative to **2a**, but the shorter bond lengths in **2** than in *N*-methylpiperidine should tend to raise the **a,e** energy gap. The nitrogen inversion barrier for **2**, 10.1 kcal/mol ($-80\text{ }^{\circ}\text{C}$) for **2e** \rightarrow **2a** from the Anet equation, is similar to that for **3**, 10.4 kcal/mol ($-80\text{ }^{\circ}\text{C}$) for **3e** \rightarrow **3a** from peak coalescence. Both are significantly higher than the 9.0 kcal/mol ($-70\text{ }^{\circ}\text{C}$) for **1**, which is reasonable considering the greater ground state steric hindrance in the bicyclic system **1**.

The ring reversal barriers, 11.2 kcal/mol ($-80\text{ }^{\circ}\text{C}$) by peak coalescence for **2e'** \rightarrow **2a** and 9.1 kcal/mol ($-80\text{ }^{\circ}\text{C}$) from the Anet equation for **3e'** \rightarrow **3a**, are both significantly higher than those for "nonpassing" tetraalkylhydrazines, but lower than those for "passing" barriers. These results suggest that there may be some residual NN^+ electronic interaction and that rotation about an NN^+ bond might prove to be significantly more difficult than rotation about an NC bond of comparable substitution.

Conclusion. Conformational Effects of Methylating Tetraalkylhydrazines

The sterically most favored conformations **2e/2e'** and **3e/3e'** predominate for the pentaalkylhydrazine cations, in contrast to the situation for their neutral tetraalkyl analogues, in which electronic interaction of the adjacent lone pairs is an important factor. Alkylation at one of the nitrogens appears to "turn off" this electronic effect. The size of the change in conformational equilibria is quite different for the two systems, as is emphasized in Figure 5. In each case the **ae** form of the neutral hydrazine is lined up with the **a** form of methylated cation, on the grounds that the steric interactions of the axial methyl are similar in the nonalkylated and alkylated case. Although alkylation clearly stabilizes the **e** form relative to the **a** form in each case, the size of the effect is nearly twice as large for the tetrahydropyridazine,

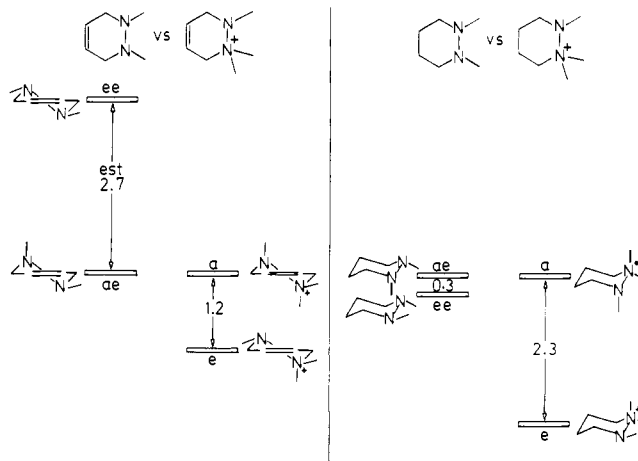


Figure 5. Comparison of conformational ground state energy differences for tetraalkyl- and pentaalkylhydrazine cations: **5** vs. **2** (right) and **6** vs. **3** (left).

about 3.9 kcal/mol,¹² than for the hexahydropyridazine, about 2.0 kcal/mol. One factor which contributes to this initially puzzling result is the amount of lone pair, lone pair electronic destabilization in the **ae** forms, which might be significantly different. The photoelectron spectroscopic lone pair, lone pair splitting of **5ae** is 1.0 eV,¹³ which is about 0.25 eV larger than for **6ae**, suggesting less lone pair, lone pair electronic interaction in the latter case which would lead to a smaller methylation effect. Another factor which cannot be ignored in considering both the PE and NMR results for **6** vs. **3**, however, is 1,3 overlap of the vinyl and lone pair electrons,¹⁴ which could well account for a couple of kcal/mol. We argue that **2** vs. **5** is a less ambiguous case for considering the electronic energy difference between *gauche* and *anti* hydrazines. In previous work we found that the electronic effect of a nearly aligned vs. a perpendicular adjacent nitrogen lone pair on the nitrogen inversion activation energy in a hydrazine is about 4 kcal/mol.³ Since this is an sp^2,sp^3 interaction, it should be larger than the sp^3,sp^3 interaction of a ground state hydrazine, so the 2 kcal/mol effect seen here is at least consistent with the inversion barrier number.

Experimental Section

1,2-Dimethyl-1-azonia-2-azabicyclo[2.2.2]octane Iodide (1) and 2,2-Dimethyl-1-aza-2-azonabicyclo[2.2.2]octane Iodide (7). Methyl iodide (0.91 mL, 14.6 mmol) was added dropwise, by syringe, over 5 min to a solution of 1.84 g (14.6 mmol) of **4** in 30 mL of dioxane. After 24 h at room temperature, the yellowish solid formed was collected by filtration and found to be a 70:30 mixture of **1** and **7** by ^1H NMR. The mixture was dissolved in a minimum volume of boiling ethanol and cooled, **7** filtered off, and the supernatant concentrated to two-thirds the original volume, cooled, and filtered. After three repetitions no more **7** was obtained upon cooling. After a final recrystallization of the combined **7** samples, 0.92 g (23.5%) of **7**, mp $235\text{--}236\text{ }^{\circ}\text{C}$, was obtained:¹⁵ ^1H NMR (D_2O) δ 1.6–1.95 (m, 4 H), 2.3 (m, 1 H), 3.1–3.3 (m, 2 H), 3.4 (s, 6 H), 3.6 (m, 2 H), 3.65–3.9 (m, 2 H); ^{13}C NMR ($\text{Me}_2\text{SO}-d_6$) δ 23.4, 24.2, 47.8, 58.8, 69.1; IR (KBr) 2850–2990, 1450–1500, 1160 cm^{-1} .

The **1** contained in the supernatant from the above crystallizations was precipitated from solution by addition of ethyl acetate to give 2.04 g (52%) of **1**: mp $221\text{--}222\text{ }^{\circ}\text{C}$ dec;¹⁵ ^1H NMR (CDCl_3) δ 2.0–2.25 (m, 4 H), 2.25–2.4 (m, 1 H), 2.9 (s, 3 H), 3.2–3.3 (m, 2 H), 3.35 (s, 3 H), 3.7–4.1 (m, 2 H), 4.2–4.5 (m, 2 H); ^{13}C NMR (CDCl_3) δ 21.4, 23.4, 40.5, 51.1, 57.6, 59.1; IR (KBr) 2800–3000, 1400–1500, 1070 cm^{-1} .

(12) The 2.7 kcal/mol estimate for **6ee** relative to **6ae** comes from low-temperature cyclic-voltammetry data and a 7 kcal/mol estimate for ring reversal in **6**. See: Nelsen, S. F.; Echegoyan, L.; Clennan, E. L.; Evans, D. H.; Corrigan, D. A. *J. Am. Chem. Soc.* **1977**, *99*, 1130. Although this number may be too high, **6ee** remains undetected by NMR, and a larger methylation effect on **6** than on **5** is certain.

(13) (a) Nelsen, S. F.; Buscheck, J. M. *J. Am. Chem. Soc.* **1974**, *96*, 6987. (b) Schweig, A.; Thon, N.; Nelsen, S. F.; Grezzo, L. A. *Ibid.* **1980**, *102*, 7438.

(14) For a discussion of such 1,3 overlaps which are large enough to see easily on an electron volt scale in bicyclic systems, see: Nelsen, S. F.; Hollinsed, W. C.; Grezzo, L. A.; Parmelee, W. P. *J. Am. Chem. Soc.* **1979**, *101*, 7347.

When the iodide of **1** was found to be too insoluble for low-temperature ^{13}C NMR work, the fluoroborate was prepared by trituration of the iodide with silver oxide and 40% tetrafluoroboric acid, washing the solids formed with acetone, concentration, and recrystallization from acetone (mp 262–263 °C dec).

1,1,2-Trimethylhexahydropyridazinium Tetrafluoroborate (2). A solution of 0.54 g (4.74 mmol) of **5** in methylene chloride was added over 10 min to a vigorously stirred suspension of 0.71 g (4.79 mmol) of trimethyloxonium tetrafluoroborate in 5 mL of methylene chloride. After the solution was stirred overnight the solvent was removed by rotary evaporation, giving 0.9 g of residue. Crystallization from ethanol-ethyl acetate gave 0.8 g (78%) of **2**: mp 274–275 °C dec; 15 ^1H NMR (acetone- d_6) δ 1.5–2.2 (m, 4 H), 2.75 (s, 3 H), 2.95–3.2 (m, 2 H), 3.3 (s, 6 H), 3.6–3.9 (m, 2 H); IR (KBr) 2860–3000, 1430–1500, 1020–1150 (BF_4^-) cm^{-1} .

1,1,2-Trimethyl-1,2,3,6-tetrahydropyridazinium Tetrafluoroborate (3). This was prepared and purified as for **2**, from 0.7 g (4.73 mmol) of trimethyloxonium tetrafluoroborate and 0.53 g (4.7 mmol) of **6**, giving 0.82 g (81%) of **3**; mp 218–219 °C dec; 15 ^1H NMR (CD_3CN) δ 2.7 (s, 3 H), 3.08 (s, 6 H), 3.51 (m, 2 H), 4.00 (m, 2 H), 5.8 (m, 2 H); IR (KBr) 3020, 2940, 1630, 1080 (BF_4^-) cm^{-1} .

Variable-Temperature NMR Experiments

Solutions of **1** and **2** were approximately 0.5 M in substrate in acetone- d_6 . A mixed solvent of 7:3 v/v acetone- d_6 /aceto-

(15) A satisfactory C, H, N analysis was obtained from Spang Microanalytical Laboratories, Eagle Harbor, MI.

nitrile- d_3 was required for the 0.25 M sample of **3** employed. The coalescence temperature data were recorded and analyzed, as in previous work, 1,3 on a Varian XL-100 spectrometer operating in the FT mode. Total line shape analysis used program NMRSIM (written by M. Chen), and activation parameters and statistical error parameters employed program DEEJAY written by G. R. Weisman. Computations were carried out on a Harris/7 computer.

The measurements of broadening at C_6 at various temperatures were carried out on a JEOL FX-200 spectrometer operating in the FT mode. The experiments on **2** (300 mg in 2.5 mL of acetone- d_6) were measured with a digital resolution of 0.06 Hz per point, and those on **3** at 0.10 Hz per point. Spectra were determined every 5 °C between –55 and –90 °C to find the point of maximum broadening, the peak width at half-height was measured visually from expanded spectra for C_6 and nonbroadened peaks, and the temperature of maximum broadening (± 2 °C) was determined from a plot of the difference vs. temperature.

Acknowledgment. We thank the National Institutes of Health for financial support under Grant GM25428 and the National Science Foundation Major Instrument program for funds used in the purchase of the spectrometers employed in this work. We also thank David F. Hillenbrand for help in using the NMR equipment.

Fluoromethyl Formate. Synthesis, Microwave Spectrum, Structure, Dipole Moment, and Anomeric Effect

Alexander D. Lopata and Robert L. Kuczkowski*

Contribution from the Department of Chemistry, The University of Michigan, Ann Arbor, Michigan 48109. Received September 19, 1980

Abstract: Eleven isotopic species of fluoromethyl formate have been synthesized. They were obtained via the decomposition of vinyl fluoride ozonide. The isotopic enrichments were consistent with the postulate that this ozonide upon decomposition produces some fluoromethyl alcohol which reacts further to give fluoromethyl formate. The isotopic species were identified by microwave spectroscopy. Transition assignments were made and rotational and centrifugal distortion constants were determined. Two excited vibrational states of the normal species were also assigned. Principal axes dipole moment components of $|\mu_a| = 0.10$ D, $|\mu_b| = 2.09$ D, and $|\mu_c| = 0.80$ D were determined. These gave a molecular dipole moment of 2.24 (2) D. The structure was determined and detailed parameters were obtained. The heavy atoms (exclusive of fluorine) have the usual *cis* ester configuration but slight deviations from exact planarity apparently occur ($\tau(\text{OCO}_2\text{C})$ is $1.5 \pm 1^\circ$). The fluorine orientation is approximately perpendicular to the formyl ester plane ($\tau(\text{FCO}_2\text{C})$ is $84 \pm 1^\circ$). This structure and its relationship to the anomeric effect are discussed.

Introduction

Recently, a simple but new compound, fluoromethyl formate (FMF), was identified in our laboratory 1 as a product from the decomposition of 3-fluoro-1,2,4-trioxolane, i.e., vinyl fluoride ozonide (VFO). During the characterization of FMF, we realized that the fluoromethyl group had an exaggerated *gauche* conformation and estimated that the FCOC dihedral angle was probably 85–90°. This conformation attracted our interest and it motivated us to obtain more detailed bond distances and angles which are reported herein.

This conformation was interesting for at least three reasons. (1) It contrasted with several other recent microwave (MW) reports involving CH_2F groups where the CF bond was coplanar with an adjacent carbonyl group (*cis*- and *trans*-fluoroacetic acid, 2 *cis*- and *trans*-fluoroacetyl fluoride, 2 *trans*-fluoromethylacetone, 3

and *cis,trans*-1,3-difluoromethylacetone. 4,5 (2) The internal rotation angle of the CH_2F groups deviated markedly from the canonical value of 60° for a *gauche* conformation. (3) The conformation could be correlated to the anomeric effect. 7

This last reason made it especially attractive to obtain more precise structural parameters. The $\text{CH}_2\text{F}-\text{O}-$ moiety (more specifically, the compound CH_2FOH) has been a prototypal model for extensive MO analyses of the anomeric effect. 7a,8 So far

(3) Saegerbarth, E.; Krisher, L. C. *J. Chem. Phys.* **1970**, *52*, 3555–3562.

(4) Finnegan, D. J.; Gillies, C. W.; Suenram, R. D.; Wilson, E. B.; Karlsson, H. *J. Mol. Spectrosc.* **1975**, *57*, 363–376.

(5) Reference 4 suggests, along with the gas-phase IR data, 6 that a *gauche,gauche* form may be more stable than the *cis,trans* configuration whose MW spectrum was assigned for $\text{CH}_2\text{FC}(\text{O})\text{CH}_2\text{F}$.

(6) Crowder, G. A.; Cook, B. R. *J. Mol. Spectrosc.* **1968**, *25*, 133–137.

(7) The literature on the anomeric effect is extensive. Two recent reports which contain excellent summaries and lists of references are (a) Wolfe, S.; Whangbo, M.-H.; Mitchell, D. *J. Carbohydr. Res.* **1979**, *69*, 1–26. (b) Szarek, W. A.; Horton, D. Eds.; "Anomeric Effect, Origin and Consequences", ACS Symposium Series No. 87; American Chemical Society: Washington, D.C., 1979.

(1) Mazur, U.; Lattimer, R. P.; Lopata, A.; Kuczkowski, R. L. *J. Org. Chem.* **1979**, *44*, 3181–3185.

(2) Van Eijck, B. P.; Brandts, P.; Maas, J. P. M. *J. Mol. Struct.* **1978**, *44*, 1–13.